Title: **Functional MRI with active, fully implanted, deep brain stimulation systems: safety and experimental confounds**

Authors: David W Carmichael[1], Serge Pinto[2], Patricia Limousin-Dowsey[2], Stephane Thobois[2], Philip J Allen[3], Louis Lemieux[1], Tarek Yousry[4], John S Thornton[4]

[1]Department of Clinical and Experimental Epilepsy, Institute of Neurology, University College London, London, UK
[2]Sobell Department of Motor Neuroscience and Movement Disorders, Institute of Neurology, University College London, London, UK
[3]Department of Clinical Neurophysiology, National Hospital for Neurology and Neurosurgery, London, UK
[4]Lysholm Department of Neuroradiology, National Hospital for Neurology and Neurosurgery, London, UK

Correspondence to:

David Carmichael PhD MInstP
Wellcome High Field MR Research Laboratory
University College London
12 Queen Square
London WC1N 3AR
Tel +44 (0)20 76762006
Fax +44 (0)20 76762005
email d.carmichael@ion.ucl.ac.uk

Abstract

We investigated safety issues and potential experimental confounds when performing functional magnetic resonance imaging (fMRI) investigations in human subjects with fully implanted, active, deep brain stimulation (DBS) systems. Measurements of temperature and induced voltage were performed in an *in vitro* arrangement simulating bilateral DBS during magnetic resonance imaging (MRI) using head transmit coils in both 1.5 and 3.0T MRI systems. For MRI sequences typical of an fMRI study with coil-averaged specific absorption rates (SARs) less than 0.4 W/Kg, no MRI-induced temperature change greater than the measurement sensitivity (0.1ºC) was detected at 1.5T, and at 3T temperature elevations were less than 0.5ºC, i.e. within safe limits. For the purposes of demonstration, MRI pulse sequences with SARs of 1.45 W/Kg and 2.34 W/kg (at 1.5T and 3T respectively) were prescribed and elicited temperature increases (>1ºC) greater than those considered safe for human subjects. Temperature increases were independent of the presence or absence of active stimulator pulsing. At both field strengths during echo planar MRI the perturbations of DBS equipment performance were sufficiently slight, and temperature increases sufficiently low to suggest that thermal or electromagnetically mediated experimental confounds to fMRI with DBS are unlikely. We conclude that fMRI studies performed in subjects with subcutaneously implanted DBS units can be both safe and free from DBS-specific experimental confounds. Furthermore, fMRI in subjects with fully-implanted rather than externalised DBS stimulator units may offer a significant safety advantage. Further studies are required to determine the safety of MRI with DBS for other MRI systems, transmit-coil configurations and DBS arrangements.

Introduction

Deep brain stimulation (DBS) effected using implantable neurostimulation systems has become an important symptomatic therapy in movement disorders such as Parkinson's disease (Limousin 1995, Volkmann 1998, DBS PD study group 2001). The technique typically involves high-frequency electrical stimulation of the subthalamic nucleus using surgically implanted electrodes connected via subcutaneous extension leads to an implantable pulse generator (IPG) commonly located subcutaneously in the pectoral area.

Despite its success, the precise neurophysiological mechanisms underlying the efficacy of DBS therapy remain a subject of debate (Dostrovsky 2002, McIntyre 2004, Goerendt 2006). Functional brain imaging performed concurrently with DBS may help to clarify these issues and furthermore the potential of DBS to selectively and reversibly modulate basal ganglia-thalamocortical circuits during imaging studies offers a unique investigative opportunity (Georgi 2004, Hesselmann 2004, Jech 2001, Stefurak 2003). Since the first functional imaging investigation of DBS using positron emission tomography (PET) (Limousin 1997) numerous PET and single photon emission computed tomography (SPECT) studies have been reported (e.g. Fukuda 2001, Grafton 2006, Hilker 2004, Pinto 2004, Schroeder 2003, Thobois 2002).

In contrast to the popularity of PET/SPECT studies, to date functional magnetic resonance imaging (fMRI) studies performed with active DBS have been limited in number and particularly in the numbers of subjects studied (Rezai 1999, Jech 2001, Stefurak 2003, Hesselmann 2004, Arantes 2006, Phillips 2006). This is despite the potential advantages of fMRI as compared to PET (wider availability, improved spatial and temporal resolution, and absence of radioactive pharmaceuticals) and is largely a consequence of concerns regarding the safety of both MRI in the presence of metallic implants (Rezai 2005), and the possible effects of the MRI scanner electromagnetic fields upon IPG function. Thus far, fMRI of DBS has been limited to subjects with externalised IPGs, allowing the IPG to be located remotely from the MRI scanner, and only one recent study (Phillips 2006) has been performed at a magnetic field strength greater than 1.5T.

Studies with externalised IPGs are usually performed within a short time of the electrode implantation procedure, before the IPG and electrode extension leads are sited subcutaneously. There are a number of potential advantages in the context of imaging neuroscience to scanning subjects with fully implanted, rather than externalised, IPGs: the acute effects of the surgery may be separated from those of chronic stimulation, the population from which suitable volunteer subjects may be recruited is larger, subjects may be

selected for whom the efficacy of DBS therapy has been established and well characterized, and finally, longitudinal studies to monitor the long term effects of DBS are possible.

The predominant safety concern with MRI in DBS patients is a potential rapid and harmful increase in tissue temperature close to the electrode tips due to focusing of the scanner radiofrequency (RF) field (Pictet et al, 2002, Rezai 2002, Rezai 2005). Indeed severe patient injuries have been reported when safe operating procedures have not been correctly followed (Speigel 2003, Utti 2002). Additionally, voltages induced in the DBS circuit during MRI may, if of sufficient magnitude, cause direct injury or uncontrolled neural stimulation. Despite these concerns it is generally accepted that clinical MRI examinations of patients with inactive implanted DBS systems are safe, provided safety guidelines are observed (e.g. low RF specific absorption rate (SAR) pulse sequences at 1.5T only, a head transmit/receive coil, and the IPG output set to off and 0V (Shellock 2005, Rezai 2004)). Both active DBS during fMRI, and fMRI performed at 3T with the goal of exploiting the increased sensitivity available contravene these guidelines and so additional system-specific safety testing is required.

Assuming safety can be established, any experimental complications arising from DBS during fMRI must be addressed. Firstly, for active DBS, the effect of the MRI electromagnetic fields upon IPG function and hence accurate stimulus delivery is a concern. An altered or interrupted stimulus delivery could confound an fMRI study, cause discomfort to the subject and potentially damage to the IPG. Secondly, with regard to heating; any externally induced increases in tissue temperature, even if safe (i.e. too low to cause tissue damage), may still compromise fMRI studies since elevated cerebral temperature may cause local CBF to increase independently of functional activation as part of the physiological thermoregulatory response (Salcman 1989, Collins 2004). Changes in regional cerebral metabolism associated with temperature elevations might also be sufficient to perturb the efficacy of DBS itself. In addition to such physiological changes, induced temperature deviations may cause direct alterations in image intensity due to the thermal dependence of the magnetic resonance properties of tissue. As a consequence of these factors, if the degree of heating is dependant on the presence or otherwise of active stimulation, such intensity changes may cause artefactual activation patterns when comparing the “on” versus “off” DBS conditions.

The purpose of the present study was to investigate safety and potential confounds when performing fMRI in subjects with fully implanted DBS systems at both 1.5Tand 3T, a field strength for which the safety of DBS has, to date, been less well established. We were particularly concerned with establishing the implications of active delivery of stimulation

pulses during fMRI. Measurements were performed using a tissue-simulating test object comparing temperature and induced voltage measurements under the contrasting conditions of “stimulator on” versus “stimulator off”.

Methods

Experimental arrangement

Following the method of Rezai at al. (Rezai 2002), a phantom was formed from poly-methyl-methacrylate (“Perspex”), (Lucite International, Southampton, UK) with shape and dimensions approximating those of an adult human torso (figure 1). Throughout this work left hand side (LHS) and right hand side (RHS) denote orientations in the standard radiological convention, i.e. relative to a patient (simulated by our test object) lying head-first supine in the scanner. The phantom was filled to a depth of 10 cm with a semi-liquid gel formed from distilled water, poly-acrylic acid partial sodium salt (Aldrich Chemical) and sodium chloride (8g/litre and 0.70 g/litre respectively) with electrical and thermal characteristics similar to those of human tissue (Park 2003).

A Kinetra 7428 (Medtronic Inc., Minneapolis, MN, USA) IPG was positioned to simulate surgical implantation in the subclavicular region, such that its outer casing was in electrical contact with the gel (figure 1). Two quadrupolar electrode leads (Medtronic model 3389) were positioned in a configuration similar to that required for bilateral STN stimulation and connected to the IPG using two Medtronic model 7482 extension leads (both of length 51cm).

For both MRI systems tested, the phantom was positioned in the centre of the magnet bore such that the tips of the electrodes were at the magnet isocentre (i.e. using the tips of the electrodes as a landmark), closely resembling the position of a patient-implanted DBS system relative to the MRI scanner static, RF and gradient magnetic fields. Relative to the simulated patient head, the image slice orientations were axial for the gradient-echo EPI and FSE sequences, and coronal for the 3D IR-SPGR volume acquisition.

For all measurements at both field strengths, the patient-weight, needed by the scanner software to calculate estimated SAR values, was entered as 50kg and the default manufacturer-provided RF pulse-shapes and durations for the specified pulse-sequences and software-levels were employed.

IPG Settings

The Medtronic Kinetra IPG system is designed to provide flexibility in the selection of stimulus parameters for DBS: stimulation may be unipolar, with the IPG case acting as an anode and the current return path via the body, or bipolar, with adjacent electrode contacts acting as respective cathode and anode. The frequency, pulse width and pulse amplitude are programmable, allowing patient-specific settings, tailored to provide maximum therapeutic benefit whilst minimizing negative side-effects (Volkmann 2002, Kuncel 2004). Due to the practical constraints of time, from the numerous permutations of possible stimulus parameters, we chose to employ a representative configuration typical of that employed in PD therapy i.e. unipolar stimulation with pulse width 60μs, frequency 130Hz, and amplitude 3V (Ashkan 2004).

Each lead provides 4 electrode contact points each of 1.5mm in length arranged linearly, separated by 0.5 mm and starting 1.5mm from the distal electrode end. Stimulation pulses as detailed above were applied to the most distal electrode contacts for both the left-hand side (LHS) and right-hand side (RHS) lead (labelled electrode contacts 4 and 0 in our arrangement (figure 1)). Four stimulation regimes were investigated: 1) bilateral stimulation (electrode contacts 0 = 3V and 4 = 3V), 2) unilateral stimulation via the RHS electrode (i.e. electrode contact 0 = 3V, contact 4 = 0V), 3) IPG set to "off", 4) IPG set to "off" and the balanced probe disconnected. Experiments 1-3 assessed the safety of MRI with the stimulator in the different modes of operation. Experiment 4 tested the degree to which the interaction of the DBS system with the MRI electromagnetic fields was perturbed by the presence of the voltage probes. Prior to and following MR scanning the DBS system was tested for normal operation outside the MRI scanner room using the inbuilt telemetry facility.

Voltage measurement

For experiments 1-3, a balanced coaxial probe was employed (Smith DC, 1993, Lemieux 1997) consisting of two 20:1 'low impedance' probes (950Ω resistors in series with 50Ω coaxial cables), with shields from each probe periodically joined to minimise ground loops, connected to a 200 MHz digital oscilloscope (Tektronix TDS 2022, Tektronix Inc., Beaverton, OR, USA) configured with differential inputs. Voltages were measured between a contact point on the IPG case surface (anode) and the connection point for electrode 0 at the proximal end of the RHS extension lead (figure 1).

In order to assess the contribution of signals induced in the test-leads to the total voltages detected, a "null" measurement was performed in which the ends of the balanced probes were connected directly together while leaving both connected to the IPG case.

Temperature measurement

Temperature data were obtained simultaneously from 4 positions using an MRI-compatible fluoroptic thermometer (Model 3100, Luxtron Corporation, Santa Clara, CA, USA; accuracy ±0.1ºC). Temperature was recorded every 2-3s from sensors sited at electrode contacts 0 and 4, the IPG case, and from a reference point at the centre of the phantom 'head' remote from the electrode contacts. The contacts at the ends of the electrode leads were presumed the site of maximal temperature change (Pictet et al, 2002, Achenbach 1997). Temperature changes relative to the pre-scan baseline value are reported, the baseline value being the mean of 10 measurements obtained immediately prior to the pre-scan acquisition for each image set.

1.5T imaging

Data were acquired using a 1.5T GE Signa Horizon LX MRI system (software level 9.1) (GE Healthcare Technologies, Waukesha, Wisconsin, USA) with the standard transmit/receive birdcage head coil and a standard whole-body gradient set with maximum gradient strength 23mT/m and slew rate 120T/m/s. Four MRI sequences were investigated: a high-SAR fast spin-echo (FSE) sequence, a 3-plane gradient-echo localiser, a T1-weighted structural volume acquisition (3D IR-prepared spoilt gradient echo (IR-SPGR)) and a gradient-echo echo-planar imaging (EPI) time series. The latter three acquisitions were representative of those commonly used in fMRI studies; the FSE sequence was used to generate heating sufficient to allow accurate comparison of the effects of the stimulator settings (experiments 1-3 above) upon temperature elevation. Sequence details are given in table 1.

3T imaging

Measurements were performed on a General Electric 3T Excite MRI system (software level 12_M4) again using the manufacturer's transmit/receive birdcage head coil and in this case a head gradient coil set (maximum gradient strength 50mT/m; slew rate 150T/m/s). Four imaging sequences (table 1) similar to those employed at 1.5T were investigated.

Results

Temperature

Typical temperatures at the reference position within the gel positioned in the magnet bore at the start of an experiment were between 15-17ºC. Temperature changes are summarised in table 1. At 1.5T no temperature rise was detected for the 3 plane-localiser, structural, or EPI sequences. For the FSE sequence the maximum temperature increase (ΔT) measured was 1.4ºC at the tip of the LHS electrode (contact 4). At 3T there was a measurable ΔT for all the

sequences with a maximum again at the tip of the LHS electrode (contact 4) of 0.5ºC for the structural sequence, 0.4ºC for the localiser and 0.2ºC for EPI.

At the electrode contacts, the differences in maximum temperature change between the different stimulator conditions lay within the measurement sensitivity (compare background temperature fluctuations seen at the reference position to differences at the electrode contacts in figure 2) and so no formal statistical tests were performed.

Figure 2 shows the ΔT from baseline during the FSE sequence for the 1.5T (a-d) and 3T systems (e-h). For each scanner the temperature obtained at each measurement position is plotted for each of experiments 1-4. In figures 2a, 2b, 2e & 2f the temperature at the electrode contacts is shown. The ΔT were independent of the stimulator settings (experiments 1-3) and furthermore, when the equipment used to monitor the IPG output was disconnected (experiment 3), ΔT was not affected. At both field strengths ΔT at the LHS electrode was more than 4 times that for the RHS electrode (figs. 2a, 2e; 2b, 2f). In order to eliminate the possibility of this asymmetry being due to a faulty temperature sensor, the FSE sequence was run for a second time at 3T with the temperature sensors for each electrode interchanged; ΔT at each of the electrodes was unchanged from the original configuration. Figures 2c, 2d, 2g & 2h, show ΔT at the IPG case and the central reference. There was no measurable temperature rise at either of these locations during any experiment.

Voltage

Figure 3 shows voltage measured between one active IPG output connection and the IPG case during the EPI acquisition at 1.5T. Three distinct signal components were seen: the IPG pulses, aliased high frequency signals arising from the MRI RF pulses and low frequency voltages due to the switched imaging gradients. The 60μs width stimulator pulses contained only 1-2 points at the oscilloscope sampling rate (40μs per point) and the output pulse amplitudes for a nominal 3V setting were 2.4V; this amplitude reduction was found to occur only when the IPG case contacted the phantom gel, and is likely due to the reduced total load impedance provided by the return current path through the gel in parallel with the low-impedance voltage probes. Radio frequency signals corresponding to the fat-suppression and slice-selective 90^{o} pulses of the EPI MRI sequence were seen with peak-to-peak (pk-pk) levels of close to 5V, and, subsequent to these, smaller (<1.2V) spikes associated with the EPI read and phase gradient switching.

Similar results were obtained at 3T (figure 4a), with 9V pk-pk RF pulses which were higher than, and gradient-switching induced voltages (less than 0.5V) which were less than those

seen at 1.5T (c.f. figures 3a and 4a), despite the higher gradient strengths and slew rate of the 3T system.

To assess the proportion of the observed signals that were contributed by voltages induced in the measurement circuit leads, as opposed to the DBS circuit in isolation, a null experiment was performed at 1.5T in which the balanced probe was shorted by connecting both contacts to the IPG case. No IPG, but both RF and gradient-switching signals were seen. The RF pulse amplitude was approximately 25% of that in figure 3, suggesting that the majority of the RF field signal was induced in the DBS circuit rather than in the test leads. In contrast, the gradient-switching spikes were similar in amplitude to those in figure 3, suggesting that nearly all of these signals were induced in the section of the circuit associated with the test leads, rather than the DBS circuit itself.

In the majority of our recordings, the IPG maintained a continuous pulsed output with constant period and magnitude, the pulse amplitudes obtained being the sum of the original IPG pulse and the MRI-induced signals. However, on both MRI systems, disturbances to the period of the DBS pulses were occasionally (less than 1 in 10 recordings) observed (figures 3b and 4b): subsequent to the MRI RF pulses, and during the rapid read-out gradient switching, a single extended period between IPG pulses was seen, after which the pulse train continued at the original frequency. This extended period was always approximately 50% longer than the normal duration.

Induced voltages of similar magnitudes were obtained at both field strengths for the other MRI sequences tested. The maximum induced voltages observed at either field strength during any sequence were less than 20V.

Discussion

Safety of active DBS during fMRI

Guidelines

Current UK (MDA 2003) and similar international (IEC 2002) guidelines suggest that MRI-induced heating should not cause cerebral temperature to exceed 38ºC, implying temperature elevation in the brain should be less than 1ºC. Guidelines (ICNIRP 2003) for exposure to electromagnetic fields in the 100-1000Hz frequency range, typical of both DBS and MRI gradient-switching induced signals, suggest a maximum charge density (calculated by dividing the product of the voltage and pulse width by the product of the impedance and surface area) of 30μC/cm^2. It has been determined that chronic DBS using pulses of

magnitude 1-4.4V, duration 60-210us, and frequency 130-185 Hz complies with this limit and causes no tissue injury (Haberler 2000, Burbaud 2002, Kuncel 2004).

Temperature

The overall rate of dissipation of heat from the gel phantom relies on the difference in its temperature from that of the surroundings making it necessary to achieve thermal equilibrium prior to measurements. Our particular concern was to detect local heating concentrated around the electrodes where the principle mechanism for heat dissipation is thermal conduction and convection within the phantom gel itself. The thermal and electrical properties of the gel at room temperature simulate those of human tissue at 37ºC (Park et al 2003). It is noteworthy that temperature changes recorded in a gel-filled phantom represent conservative, worse case, estimates of tissue heating, since in vivo temperature elevations would be reduced by cerebral blood flow (CBF) (Salcman 1989, Collins 2004). Here, scan durations used were typical of fMRI sequences: higher peak temperatures would be expected for longer scan durations. As in other studies (e.g. Bhidayasiri 2005, Georgi 2004, Rezai 2002), where significant heating was observed it occurred quickly, within 30 seconds of scan commencement.

We investigated heating due to both typical fMRI protocols and a high SAR FSE sequence prescribed with the deliberate intention of generating sufficient heating for accurate determination of the effects of IPG settings upon ΔT. On the 1.5T system this high SAR sequence produced a maximum ΔT of 1.4ºC, whereas for the fMRI sequences (localiser, 3D IR-SPGR and GE-EPI) ΔT remained below the measurement sensitivity of our thermometry system (0.1ºC) implying a factor of 10 safety margin for compliance with the safety guidelines. At 3T, the high-SAR FSE sequence produced a maximum ΔT of 2.2ºC; for the other acquisitions the maximum ΔT, i.e. 0.5ºC for the 3D IR-SPGR sequence, lay comfortably within the permissible range, implying a factor of 2 safety margin for compliance with the safety guidelines. It should be noted that while these factors indicate a relative level of safety between similar protocols at 1.5T and 3T they should not be used directly to infer safety in a patient study.

Temperature elevations for comparable MRI pulse sequences were higher for the 3T system, where SAR values reported by the scanner software were also higher than at 1.5T**,** consistent with the known field-dependence of RF power deposition. Although it is expected that interactions between the DBS circuit and the RF field should be frequency, and therefore field strength dependent, this does not imply that the risk of thermal injury increases with increasing field strength *per se*. It should be noted that the software-reported SAR values

from the particular systems used were independent of RF calibrations obtained during pre-scanning. This avoided any inaccuracy due to inter-scan re-calibration e.g. between different DBS settings. However this complication should be considered when performing experiments or patient studies on other systems where reported SAR values may be influenced by re-calibration. Importantly, the algorithms used to estimate SAR may differ between MRI systems, even those from the same manufacturer (Baker et al 2004), making relative predictions of tissue heating based on SAR values uncertain.

Changing the IPG settings between inactive, active unilateral and active bilateral stimulation (experiments1-3) made no detectable difference to ΔT for any of the MRI sequences on either MRI system, indicating that periods of active stimulation during MRI provide no additional safety risks with respect to tissue heating.

For both MRI systems, where a significant ΔT was detected, the difference in ΔT obtained between the bilateral electrode contacts was large; the LHS electrode temperature increased approximately 4 times more than that of the RHS electrode. An asymmetry in ΔT for RHS and LHS electrodes has been reported previously (Baker 2004, Bhidayasiri 2005) and is likely to reflect the asymmetry in the DBS circuit with respect to the scanner RF field orientation. Significantly different local conditions at the tips of the RHS and LHS are unlikely because the gel was highly uniform and our observations were reproducible despite effective remixing of the gel around the electrodes as the temperature probe was repositioned.

Our observations with regard to temperature for *active* DBS during MRI performed at 1.5T with a transmit/receive head coil are consistent with previous studies performed at this field strength with the IPG *inactive* (Finelli 2002, Rezai 2002). Those authors concluded that, with appropriate precautions, MRI was safe in patients with implanted DBS systems. Our results both confirm this, and suggest that active DBS does not add any significant risk due to RF heating. This may be important in clinical practice, where it may be advantageous to patients to maintain their stimulation regime during clinically indicated MRI examinations, in contrast to the current practice of setting the IPG output to OFF and 0V prior to MRI.

A recent study (Phillips 2006) also addressed the safety of fMRI with active DBS at 3T, notable differences from the present work being the use of an MRI system from a different manufacturer with presumably different RF coil geometry and SAR calculation method, and an externalised IPG located remotely from the MRI magnet. These authors reported a similar temperature rise to that reported herein for a 3D magnetization-prepared gradient-echo sequence, and a mean temperature rise of 0.6^0C for a gradient-echo fMRI EPI sequence

(SAR 0.6W/Kg). In contradistinction to our results, the maximal temperature increase of 1.36^0C was apparently dependent upon the presence or absence of stimulation. The disparity with our results may be attributed to the presence of the extended IPG extension lead in their case. While the temperature rises reported were considered acceptable from the point of view of safety, we have shown that using a transmit/receive head coil and a fully implanted DBS system produces smaller ΔT at the electrode contacts independent of stimulator activity for a similar fMRI EPI pulse sequence at 3T.

Voltage

A system was devised to provide reliable measurement of voltages in the DBS circuit in the presence of the MRI electromagnetic fields. Both RF and low frequency gradient-switching related signals were observed. Voltages with frequency greater than 100kHz are not expected to produce direct neuronal stimulation (ICNIRP 2003) and therefore the principle hazard due to induced RF pulses is tissue heating as already addressed above. As regards the lower frequency components due to gradient-switching these were less than 0.5V and 1.2V for the 3T and 1.5T systems respectively, and our "null" measurement at 1.5T suggested that vast majority of this signal was induced in the voltage measurement leads rather than the DBS circuit itself. This is consistent with the lower voltages observed at 3T (despite the stronger, faster gradient performance), since the smaller active volume of the 3T head-gradient set resulted in less magnetic flux density linked with the voltage measurement circuit compared to the 1.5T whole-body gradient coils. We conclude that any voltages induced in the DBS circuit by gradient-switching are of a level insufficient to cause neuronal damage since the product of pulse width and voltage, and therefore charge density, was small compared to that of the DBS stimulation pulses already known to be safe.

Other safety considerations

We did not find significant effects upon RF heating due to the presence or absence of active stimulation for our simulation of the specific geometric arrangement DBS equipment typical of that employed clinically at our institution. It is possible that a different configuration of the leads and electrodes might produce a different result but this would seem unlikely since, despite the lack of dependence upon IPG function observed, significant RF heating and induced voltage amplitudes were elicited in our experiments.

Of necessity this study was limited to an investigation of pulse-sequences and scan prescriptions typical of those used in fMRI studies, i.e. predominantly axial-plane oriented images. Changes in scan orientation (keeping the number of slices and echoes, and therefore RF pulse timing, constant) are unlikely to affect temperature changes significantly

since the RF-field and resulting SAR distribution remain unchanged. However, resultant differences in the combined gradient field strengths and orientations could in turn influence the magnitude of gradient-induced voltages within the DBS circuit. Large deviations in scan geometry may therefore require specific tests to preclude the possibility of IPG malfunction.

It is instructive to compare our observations with those reported for an alternative arrangement by Georgi et al (Georgi 2004) which simulated an extracorporeal IPG situated remote from a 1.5T scanner bore and connected to the electrodes via lengthy extension leads. When these were positioned along the z-axis of the scanner, RF-induced voltages were similar to those obtained by us, and temperature rises were less than 1^0C for all sequences tested. However, with the leads in close proximity to the MRI body-transmit coil, very large, potentially hazardous induced voltages (>2000V) were recorded together with temperature elevations in excess of 40 ^{0}C. Our arrangement was very different: a head transmit/receive coil was used and the IPG, extensions and electrode leads modelled as being fixed in position subcutaneously. As for a patient, the phantom was positioned in the centre of the RF coil, minimising coupling between the RF field and the DBS system. Such a setup with a fully subcutaneous DBS system virtually eliminates the possibility of accidental placement of the DBS leads in an unfavourable position proximal to the MRI RF coil; we therefore propose that when a head coil is used for RF excitation, MRI with fully implanted DBS systems may be intrinsically less hazardous than studies performed with an externalised, remotely connected IPG.

The IPG model employed has been previously shown safe with regard to torque and magnetic displacement force at both 1.5 and 3T (Baker, 2005). We did not investigate 'fault' conditions such as hazards due to fractured lead connections (Georgi 2004). The DBS stimulator was checked for normal operation using the Medtronic Programmer before and after all measurements. Such checks before any MRI study are prudent to eliminate the possibility of potentially hazardous faults in the DBS circuit. The IPG was exposed to static, RF and switched-gradient magnetic fields over long periods in our experiments without damage or the occurrence of reprogramming.

Active DBS and fMRI: potential confounds

IPG Function

For a proper fMRI study of the neurofunctional mechanisms and correlates of DBS it must be established that the IPG functions exactly as required during the MRI acquisitions. As in a previous report (Tronnier 1999), in our study the IPG maintained a continuous pulsed output during all MRI sequences and, was never seen to automatically switch off. However, spontaneous IPG switching off/on during MRI has been observed (Georgi 2004), and we did notice such effects in pilot experiments using an IPG with a partially exhausted battery (less than 50% full charge). In the majority of our measurements on both scanners during EPI the IPG pulse output was identical to that obtained with the scanner inactive, apart from superposition of the induced voltages described. Less than 10% of our measurements demonstrated stretching by 50% of a single inter-pulse interval shortly after a 90^{o} RF pulse, after which pulsing continued with the correct inter-pulse duration. The pulse amplitudes remained unchanged. In a typical fMRI acquisition, since the repetition frequency of the RF pulses is approximately $1/10^{th}$ of the stimulator pulse frequency, our results suggest that only 1 in 100 stimulator pulses could be affected. Such perturbations of the stimulator output have not been reported previously, although they are unlikely to impact significantly upon the efficacy or mechanisms of DBS and hence compromise an fMRI study. We recommend that the IPG battery level be checked prior to an fMRI study, and measurements only proceed provided that a battery level greater than 50% of maximum is available.

RF Heating

As already noted, local externally induced increases in tissue temperature may confound, or at least complicate the interpretation of fMRI with DBS, the ramifications being more severe if the degree of heating depends upon the presence or absence of active stimulation. With our experimental arrangement we observed no dependence of ΔT upon the presence or absence of stimulation pulses at either field strength. However, such a dependence was recently reported in a different setup (Phillips 2006) and, in addition to the complications already discussed, implies a concomitant difference in the RF field distribution between the 2 conditions with an associated effect upon MRI image intensity. While it is not clear whether the observation of Philips *et al.* was a measurement artefact or a real effect, it is clearly prudent to as far as possible eliminate local tissue temperature changes by suitable experimental design. We have shown that this should be possible at both 1.5T and 3T when subjects with fully implanted DBS systems are studied with a head RF transmit coil. The absence of a measurable temperature change at 1.5T should eliminate any additional

temperature-driven perfusion changes, making DBS-fMRI more straight-forward at this field strength.

Induced Voltages

The induced RF pulses observed were at frequencies (approximately 64MHz and 128Mhz at 1.5T and 3T respectively) considered too high to produce direct neuronal stimulation. We concluded, in agreement with a previous author (Georgi 2004), that any lower frequency signals induced in the DBS circuit independent of the voltage measurement apparatus during MRI were of a very low level: below the threshold required for neurostimulation effects. Therefore voltages induced in an implanted DBS system during fMRI are unlikely to present any additional experimental confounds.

Conclusions

Our results suggest that fMRI protocols which include localiser, 3D gradient-echo structural and EPI functional acquisitions can be safely performed in subjects with subcutaneously implanted DBS electrodes, leads and IPG units, with or without active stimulation at both 1.5 and 3T. No RF-induced heating was detected with these sequences in our 1.5T scanner and temperature elevations at 3T lay within safe limits. No damage to or reprogramming of the IPG occurred and only minor, physiologically insignificant perturbations in IPG performance were observed.

Confounds to fMRI experiments due to DBS are unlikely at 1.5T, since no temperature increases during EPI were detected in our arrangement with or without active stimulation, while at 3T the small temperature change observed was independent of stimulator activity. Low frequency voltages induced in the DBS circuit during MRI were in all cases below the thresholds for direct neuronal stimulation.

Heating exceeding safety guidelines was produced using the high SAR FSE sequence. Such sequences, used here for experimental purposes, should not be used in patient studies.

While we believe the physical arrangement tested is typical of that likely in fMRI of subjects undergoing DBS, any change in the geometric relationship between the DBS system components and the scanner RF and gradient coils may influence both RF heating and induced voltages and therefore IPG function. Experimenters should be aware that such changes may arise as a result of variations in the positioning of the DBS electrodes and leads between individual patients, or unavoidable deviations from a standard supine patient

position relative to the scanner bore which may be necessary for instance for PD patients with cyphosis.

Any alteration in surgical procedure (e.g. different lead geometry), or changes in the exact position of the subject within the scanner may modify the results, and substantially different arrangements would require specific safety investigations. Adjustments to the experimental protocol such as a longer duration or increasing the number of slices could modify the temperature change. In any case, it is prudent to allow a sufficient safety margin that inter-patient variability in DBS system configuration, scanning geometry and coil loading cannot elicit temperature changes that exceed the guidelines. To maximise the safety margin, we recommend adherence to strict SAR limits, the use of head RF transmit coils and performing studies at a field strength of 1.5T.

While these conclusions are encouraging, it must be noted that they apply only to the specific MRI systems, RF transmit coils, pulse sequences, RF waveforms, DBS equipment and experimental arrangement employed herein. In particular, the use of a whole-body RF transmit coil may be significantly more dangerous (Rezai 2005, Georgi 2004). The important necessity to generalise these results for application to other pulse-sequences, scanner models and MRI system manufacturers will require further experiments. A local safety assessment and strict adherence to a fixed experimental protocol are essential if MRI is to be performed safely in subjects with implants such as those required for DBS.

Acknowledgments

Oliver Josephs, Ralf Deichmann, Mark Symms, Rebecca Samson, Robert Turner, Anthony Pullen, John Wyatt and Marwan Hariz are acknowledged for their technical assistance, useful discussions and generous loans of equipment. This work was funded in part by a grant from the Medical Research Council (#G0301067). LL is supported by the Wellcome Trust (programme grant #G67176).

References

Achenbach S, Moshage W, Diem B, Bieberle T, Schibgilla V, Bachmann K: Effects of magnetic resonance imaging on cardiac pacemakers and electrodes. Am Heart J 134:467–473, **1997**.

Arantes PR, Cardoso EF, Barreiros MA, Teixeira MJ, Goncalves MR, Barbosa ER, Sukwinder SS, Leite CC, Amaro E Jr. **2006.** Performing functional magnetic resonance imaging in patients with Parkinson's disease treated with deep brain stimulation. Mov Disord. 21(8):1154-62.

Ashkan K, Wallace B, Bell BA, Benabid AL, **2004.** Deep brain stimulation of the subthalamic nucleus in Parkinson's disease 1993-2003: where are we 10 years on? Br J Neurosurg. Feb;18(1):19-34.

Baker KB, Tkach JA, Nyenhuis JA, Phillips M, Shellock FG, Gonzalez-Martinez J, Rezai AR, **2004.** Evaluation of specific absorption rate as a dosimeter of MRI-related implant heating. J Magn Reson Imaging 20:315–320.

Baker KB, Nyenhuis JA, Hrdlicka G, Rezai AR, Tkach JA, Shellock FG. **2005** Neurostimulation systems: assessment of magnetic field interactions associated with 1.5- and 3-T MR systems. J Magn Reson Imaging 21(1):72-7.

Bhidayasiri R,Bronstein JM, Sinha S, Krahl SE, Ahn S, Behnke EJ, Cohen MS, Frysinger R, Shellock FG **2005** Bilareral neurostimulation systems used for deep brain stimulation: in vitro study of MRI related heating, Magnetic Resonance Imaging, 23 (4): 549-555

Burbaud, P., Vital, A., Rougier, A., Bouillot, S., Guehl, D., Cuny, E., Ferrer, X., Lagueny, A. and Bioulac, B., **2002**. Minimal tissue damage after stimulation of the motor thalamus in a case of chorea-acanthocytosis. Neurology 59, pp. 1982–1984.

Collins CM, Smith MB, Turner R. **2004**, Model of local temperature changes in brain upon functional activation. J Appl Physiol. Dec; 97(6):2051-5.

Deep-brain stimulation for Parkinson's disease study group. 2001 Deep-brain stimulation of the subthalamic nucleus or the pars interna of the globus pallidus in Parkinson's disease. N Engl J Med. 2001 Sep 27; 345(13):956-63.

Dormont D, Cornu P, Pidoux B, Bonnet AM, Biondi A, Oppenheim C, Hasboun D, Damier P, Cuchet E, Philippon J, Agid Y, Marsault C, **1997.** Chronic thalamic stimulation with three-dimensional MR stereotactic guidance. Am J Neuroradiol 18:1093–1097.

Dostrovsky JO, Lozano AM, **2002**. Mechanisms of deep brain stimulation.
Mov Disord. 17 Suppl 3:S63-8.

Finelli DA, Rezai AR, Ruggieri P, Tkach J, Nyenhuis JA, Hrdlicka G, Sharan A, Gonzalez-Martinez J, Stypulkowski PH, Shellock FG, **2002**. MR-related heating of deep brain stimulation electrodes: An in vitro study of clinical imaging sequences. Am J Neuroradiol 23:1795–1802.

Fukuda M, Mentis MJ, Ma Y, Dhawan V, Antonini A, Lang AE, Lozano AM, Hammerstad J, Lyons K, Koller WC, Moeller JR, Eidelberg D **2001** Networks mediating the clinical effects of pallidal brain stimulation for Parkinson's disease - A PET study of resting-state glucose metabolism BRAIN 124: 1601-1609

Georgi JC, Stippich C, Tronnier VM, Heiland S, **2004**. Active deep brain stimulation during MRI: A feasibility study. Magn Reson Med 51:380–388.

Goerendt IK, Lawrence AD, Mehta MA, Stern JS, Odin P, Brooks DJ. **2006** Distributed neural actions of anti-parkinsonian therapies as revealed by PET J Neural Transm. 113(1):75-86.

Grafton ST, Turner RS, Desmurget M, Bakay R, Delong M, Vitek J, Crutcher M, **2006.** Normalizing motor-related brain activity: Subthalamic nucleus stimulation in Parkinson disease. Neurology 66: 1192 - 1199.

Hesselmann V, Sorger B, Girnus R, Lasek K, Maarouf M, Wedekind C, Bunke J, Schulte O, Krug B, Lackner K, Sturm V, **2004**. Inoperative functional MRI as a new approach to monitor deep brain stimulation in Parkinson’s disease. Eur Radiol 14:686–690.

Haberler, C., Alesch, F., Mazal, P.R., Pilz, P., Jellinger, K., Pinter, M.M., Hainfellner, J.A. and Budka, H., **2000**. No tissue damage by chronic deep brain stimulation in
Parkinson's disease. Ann Neurol 48, pp. 372–376.

Hilker R, Voges T, Weisenbach S, Kalbe E, Burghaus L, Ghaemi M, Lehrke R, Koulousakis A, Herholz K, Sturm V, Heiss WD **2004** Subthalamic nucleus stimulation restores glucose metabolism in associative and limbic cortices and in cerebellum: Evidence from a FDG-PET study in advanced Parkinson's disease. JCBFM 24 (1): 7-16.

ICNRP, 2003. Guidelines for limiting exposure to time varying electric, magnetic and electromagnetic fields (to 300GHz).

International Electrotechnical Commission (IEC), **2002** Medical electrical equipment – particular requirements for the safety of magnetic resonance equipment for medical diagnosis. IEC 60601-2-33, 1995 revised 2002.

Jech R., Urgosik D, Tintera J, Nebuzelsky A, Krasensky J, Liscak R, Roth J, Ruzicka E. **2001** Functional Magnetic Resonance Imaging During Deep Brain Stimulation: A Pilot Study in four patients with Parkinson's disease, Movement Disorders, 16(6):1126-32.

Kuncel AM, Grill WM. **2004** Selection of stimulus parameters for deep brain stimulation. Neurophysiol. Nov; 115(11):2431-41.

Lemieux L, Allen PJ, Franconi F, Symms MR, Fish DR, **1997**. Recording of EEG during fMRI experiments: patient safety. Magn Reson Med. Dec; 38(6):943-52.

Limousin, P., Pollack, P., Benazzouz, A., Hoffmann, D., Le Bas, J.F., Broussolle, E., Perret, J.E. and Benabid, A.L., **1995**. Effect on Parkinsonian signs and symptoms of bilateral subthalamic nucleus stimulation. Lancet 345, pp. 91–95.

Limousin P, Greene J, Pollak P, Rothwell J, Benabid AL, Frackowiak R **1997** Changes in cerebral activity pattern due to subthalamic nucleus or internal pallidum stimulation in Parkinson's disease ANNALS OF NEUROLOGY 42 : 283 1997

McIntyre CC, Savasta M, Kerkerian-Le Goff L, Vitek JL, **2004.** Uncovering the mechanism(s) of action of deep brain stimulation: activation, inhibition, or both.
Clin Neurophysiol. 115(6):1239-48.

MDA (Medical Devices Agency), **2003**. Guidelines for magnetic resonance equipment in clinical use with particular reference to safety; 2nd edition; Medical Devices Agency, London,

Park SM, Nyenhuis JA, Smith CD, Lim EJ, Foster KS, Baker KB, Hrdlicka G, Rezai AR, Ruggieri P, Sharan A, Shellock FG, Stypulkowski PH, Tkach J. **2003** Gelled verses Nongelled Phantom material for measurements of MRI-induced temperature increases with bioimplants. IEEE transactions on magnetics, IEEE TRANSACTIONS ON MAGNETICS 39 (5): 3367-3371

Phillips MD, Baker KB, Lowe MJ, Tkach JA, Cooper SE, Kopell BH, Rezai AR, **2006**. Parkinson disease: pattern of functional MR imaging activation during deep brain stimulation of subthalamic nucleus--initial experience. Radiology, Apr;239(1):209-16.

Pictet, Meuli R, Wicky S, van der Klink JJ.**, 2002.** Radiofrequency heating effects around resonant lengths of wire in MRI. Physics in Medicine and Biology 47(16):2973-85.

Pinto S, Thobois S, Costes N, Le Bars D, Benabid AL, Broussolle E, Pollak P, Gentil M, **2004**. Subthalamic nucleus stimulation and dysarthria in Parkinson's disease: a PET study. Brain, 127(Pt 3):602-15.

Rezai AR, Baker KB, Tkach JA, Phillips M, Hrdlicka G, Sharan AD, Nyenhuis J, Ruggieri P, Shellock FG, Henderson J. **2005.** Is magnetic resonance imaging safe for patients with neurostimulation systems used for deep brain stimulation? Neurosurgery. Nov;57(5):1056-62; discussion 1056-62.

Rezai AR, Lozano AM, Crawley AP, Joy MLG, Davis KD, Kwan CL, Dostrovsky JO, Taskar RR, Mikulis DJ, **1999**. Thalamic stimulation and functional magnetic resonance imaging: Localization of cortical and subcortical activation with implanted electrodes. J Neurosurg 90: 583-590.

Rezai AR, Finelli D, Nyenhuis JA, Hrdlicka G, Tkach J, Sharan A, Rugieri P, Stypulkowoski PH, Shellock FG, **2002**. Neurostimulation systems for deep brain stimulation: In vitro evaluation of magnetic resonance imaging-related heating at 1.5 T. J Magn Reson Imaging 15:241-250.

Rezai AR, Phillips M, Baker K, Sharan A, Nyenhuis JA, Tkach J, Henderson JM, Shellock FG, **2004**. Neurostimulation systems used for deep brain stimulation (DBS): MR safety issues and implications for failing to follow guidelines. Invest Radiol 39:300–303.

Salcman M, Moriyama E, Elsner HJ, Rossman H, Gettleman RA, Neuberth G, Corradino G, **1989** Cerebral blood flow and the thermal properties of the brain: a preliminary analysis. J Neurosurg. Apr;70(4):592-8.

Shellock FG, **2005.** Reference Manual for Magnetic Resonance Safety, Implants, and Devices: 2005 Edition. Los Angeles, Biomedical Reference Publishing Group.

Spiegel J, Fuss G, Backens M, Reith W, Magnus T, Becker G, Moringlane J-R, Dillmann U, **2003**. Transient dystonia following magnetic resonance imaging in a patient with deep brain stimulation electrodes for the treatment of Parkinson disease. J Neurosurg 99:772–774.

Smith DC, 1993 High frequency measurements and noise in electronic circuits. Van Nostrand Reinhold, New York.

Schroeder U, Kuehler A, Lange KW, Haslinger B, Tronnier VM, Krause M, Pfister R, Boecker H, Ceballos-Baumann AO Subthalamic nucleus stimulation affects a frontotemporal network: A PET study **2003** Annals of Neurology, 54 (4): 445-450

Stefurak T et al, Deep Brain Stimulation for Parkinson's Disease Dissociates Mood and Motor Circuits: A Functional MRI Case study. Movement Disorders, **2003**

Thobois S, Dominey P, Fraix V, Mertens P, Guenot M, Zimmer L, Pollak P, Benabid AL, Broussolle E, **2002**. Effects of subthalamic nucleus stimulation on actual and imagined movement in Parkinson's disease: a PET study. J Neurol. 249(12):1689-98.

Tronnier VM, Stauber A, Hahnel S, Sarem-Aslani A, **1999**. Magnetic resonance imaging with implanted neurostimulators: An in vitro and in vivo study. Neurosurgery 44:118–125.

Volkmann J, Strum V, Weiss P, Kappler J, Voges J, Koulousakis A, Lehrke R, Hefter H, Freund HJ, **1998.** Bilateral high-frequency stimulation of the internal globus pallidus in advanced Parkinson's disease. Annals of Neurology 44 (6): 953-961.

Volkmann J, Herzog J, Kopper F, Deuschl G, **2002.** Introduction to the programming of deep brain stimulators. Mov Disord.;17 Suppl 3:S181-7.

Utti RJ, Tsuboi Y, Pooley RA, Putzke JD, Turk MF, Wszolek ZK, Witte RJ, Wharen RE, **2002**. Magnetic resonance imaging and deep brain stimulation. Neurosurgery 51:1423–1431.

Figure / Table Captions

Figure 1 Schematic of the experimental set up (not to scale)

a) The phantom layout, showing the Perspex box filled with gel with the implanted DBS circuitry, voltage probe and thermometry equipment. Left hand side (LHS) and right hand side (RHS) denote orientations in the standard radiological convention, i.e. relative to a patient (simulated by our test object) lying head-first supine in the scanner.

b) Schematic viewed from above showing the voltage measurement circuit, the position and numbering of the electrode contacts, and temperature sensor positions.

Figure 2 Temperature change during the high SAR FSE sequence

a-d) Temperature change at 1.5T at different positions within the phantom, e-f) temperature change at 3T at different positions within the phantom. Temperature change was measured at positions, a & e) the LHS electrode (contact 4), b & f) the RHS electrode (contact 0), c & g) the IPG and d & h) reference position. The different IPG settings and scanning period (indicated by the horizontal bars at the top of each subfigure) are in the figure key.

Figure 3 Voltage measurements at 1.5T during EPI

a) A typical voltage measurement obtained during an EPI readout. Features are labelled a DBS pulse (1), noise from gradient switching (2), Fat saturation RF pulse (3) and RF excitation pulse (4).

b) A voltage measurement obtained during an EPI readout where the IPG output shows one delayed pulse (labelled 5).

Figure 4 Voltage measurements at 3T during EPI

a) A typical voltage measurement obtained during an EPI readout. Features are labelled a DBS pulse (1), noise from gradient switching (2), Fat saturation RF pulse (3) and RF excitation pulse (4).

b) A voltage measurement obtained during an EPI readout where the IPG output shows one delayed pulse (labelled 5).

Table 1 MRI Pulse sequence details, SAR levels and temperature changes

N.B. No temperature changes were detected at the IPG case, or at the reference position. (SAR = specific absorption rate; FSE = fast spin echo; IR-SPGR = inversion prepared spoilt gradient echo; EPI = echo planar imaging; TR = repetition time; TE = echo time; TI = inversion time; FA = flip angle; BW = receiver bandwidth; FOV = field of view; ST = slice thickness; SS = slice separation; NEX = number of excitations (averages))

Table

Scanner field strength	Pulse sequence	Sequence parameters	Average coil SAR (W/Kg)	maximum Temperature change (ºC ±0.1ºC)	
				LHS electrode tip	RHS electrode tip
1.5T	three-plane Localiser	TR 45.5 ms; TE 1.6 ms; BW 31.2 kHz; FA 30^0; FOV 24 x 24 cm; matrix 256 x 128; 15 Slices; ST 5 mm, SS 2.5 mm; NEX 1	0.01	<0.1	<0.1
	FSE	TR 4660 ms; TE 104.4; BW 31.2 kHz; FOV 24 x 18 cm; matrix 256 x 224; ETL 24; 25 slices; ST 5 mm; SS 1 mm; NEX 8;	1.45	**+1.4**	**+0.3**
	3D IR-SPGR Structural Volume	TR 14.2; TE 6.3 ms; BW 12.5 kHz; TI 650 ms; FOV 24 x 18 cm; 124 slices; ST 1.5 mm; matrix 256 x 256; NEX 1	0.05	<0.1	<0.1
	Gradient-echo EPI	TR 4000 ms, TE 40 ms, BW 62.0 kHz; FOV 19cm, matrix 64 x 64; 40 slices; ST 2mm, SS 1mm, NEX 1; 100 volumes	0.03	<0.1	<0.1
3T	three-plane Localiser	TR 4.7; TE 1.2 ms; BW 62.5 kHz ; FA 30^0; FOV 24 x 24 cm; matrix 256 x 256; 15 slices; ST 10 mm; SS 15 mm; NEX 1	0.71	**+0.4**	<0.1
	FSE	TR 6000; TE 102; BW 31.5kHz; FOV 22 x 22; matrix 512 x 256; 17 slices; ST 5 mm; SS 1.5 mm; NEX 2;	2.34	**+2.2**	**+0.6**
	3D IR-SPGR Structural Volume	TR 11.5 ms; TE 5.0 ms; BW 15.6 kHz; TI 450 ms; FOV 24 x 18 cm; 124 slices; ST 1.5 mm; matrix 256 x 256; NEX 1	0.39	**+0.5**	**+0.2**
	Gradient-echo EPI	TR 4000 ms, TE 30 ms, BW 500.0 kHz; FOV 19 x 19 cm, matrix 64 x 64; 40 slices; ST 2mm, SS 1mm, NEX 1; 100 volumes	0.16	**+0.2**	<0.1

Figure 1

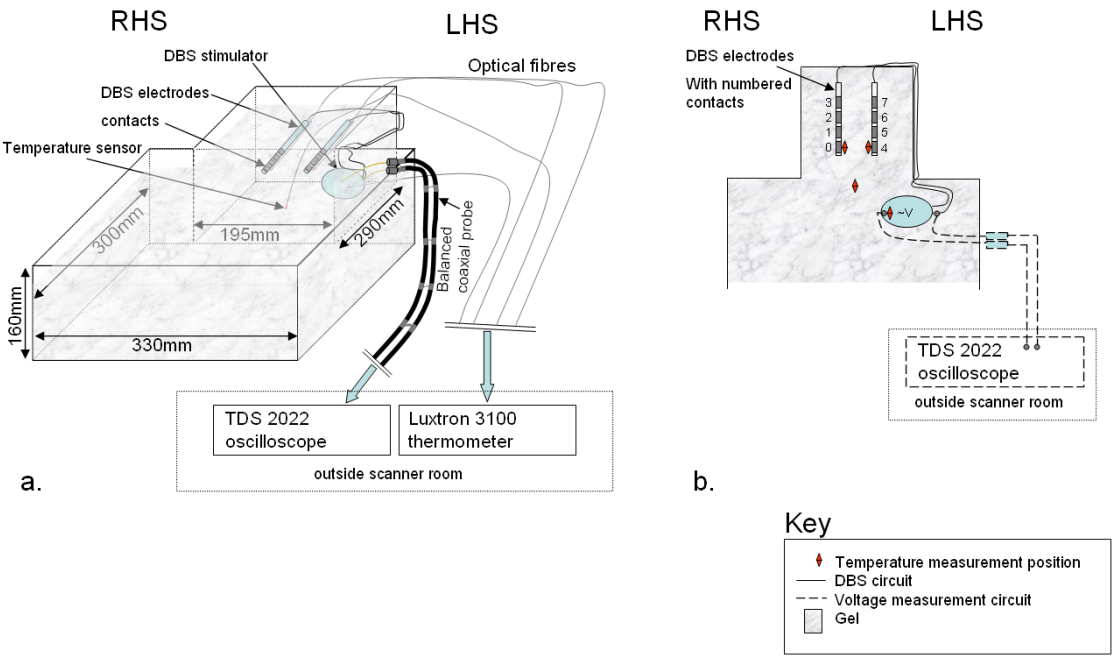
RHS
LHS
DBS stimulator
Optical fibres
DBS electrodes
contacts
Temperature sensor
300mm
195mm
290mm
Balanced coaxial probe
160mm
330mm
TDS 2022 oscilloscope
Luxtron 3100 thermometer
outside scanner room
a.
RHS
LHS
DBS electrodes
With numbered contacts
3
2
1
0
7
6
5
4
~V
TDS 2022 oscilloscope
outside scanner room
b.
Key
Temperature measurement position
DBS circuit
Voltage measurement circuit
Gel

Figure 2

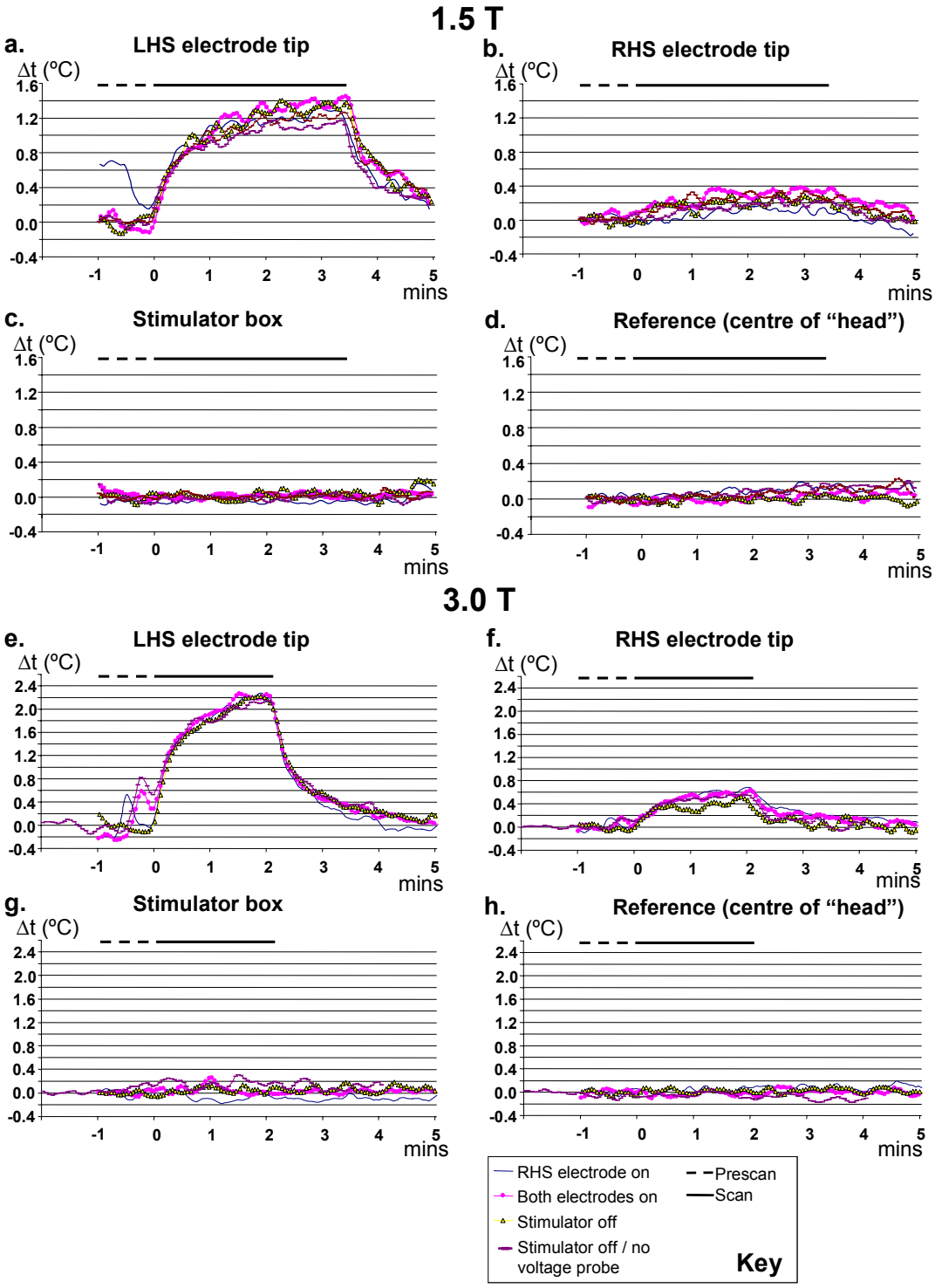
1.5 T
a.
LHS electrode tip
b.
RHS electrode tip
c.
Stimulator box
d.
Reference (centre of "head")
3.0 T
e.
LHS electrode tip
f.
RHS electrode tip
g.
Stimulator box
h.
Reference (centre of "head")
Δt (ºC)
mins
RHS electrode on
Both electrodes on
Stimulator off
Stimulator off / no voltage probe
Prescan
Scan
Key

Figure 3

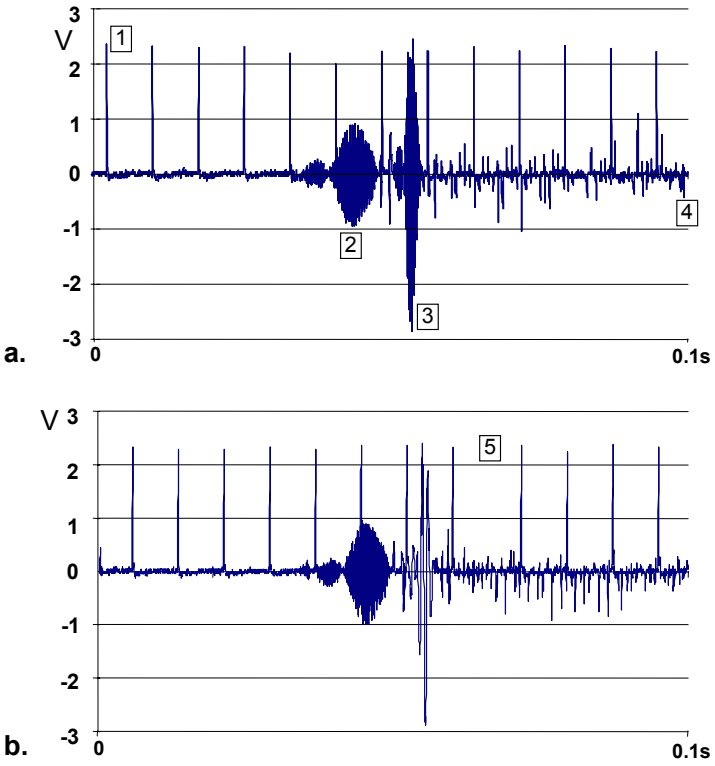

Figure 4